NeuroImage 50 (2010) 1118–1125

Contents lists available at ScienceDirect

NeuroImage

journal homepage: www.elsevier.com/locate/ynimg

Automatic search for fMRI connectivity mapping: An alternative to Granger causality testing using formal equivalences among SEM path modeling, VAR, and unified SEM

Kathleen M. Gates [a,*], Peter C.M. Molenaar [a], Frank G. Hillary [b], Nilam Ram [a], Michael J. Rovine [a]

[a] Department of Human Development and Family Studies, The Pennsylvania State University, S110 Henderson, University Park, PA, 16802, USA
[b] Department of Psychology, The Pennsylvania State University, USA

ARTICLE INFO

Article history:
Received 20 July 2009
Revised 16 November 2009
Accepted 29 December 2009
Available online 6 January 2010

ABSTRACT

Modeling the relationships among brain regions of interest (ROIs) carries unique potential to explicate how the brain orchestrates information processing. However, hurdles arise when using functional MRI data. Variation in ROI activity contains sequential dependencies and shared influences on synchronized activation. Consequently, both lagged and contemporaneous relationships must be considered for unbiased statistical parameter estimation. Identifying these relationships using a data-driven approach could guide theory-building regarding integrated processing. The present paper demonstrates how the unified SEM attends to both lagged and contemporaneous influences on ROI activity. Additionally, this paper offers an approach akin to Granger causality testing, Lagrange multiplier testing, for statistically identifying directional influence among ROIs and employs this approach using an automatic search procedure to arrive at the optimal model. Rationale for this equivalence is offered by explicating the formal relationships among path modeling, vector autoregression, and unified SEM. When applied to simulated data, biases in estimates which do not consider both lagged and contemporaneous paths become apparent. Finally, the use of unified SEM with the automatic search procedure is applied to an empirical data example.

Introduction

Connectivity mapping provides insight into how the brain orchestrates information processing. "Effective connectivity" maps in particular glean valuable information by identifying the influence that one region of interest's (ROI) activity may have on another (Friston and Stephan, 2007). In this manner, effective connectivity mapping attempts to establish causal directions of regional activity. The majority of current statistical techniques for assessing effective connectivity with functional MRI data identify either contemporaneous or lagged effects, which is problematic since both must be considered simultaneously for unbiased estimation.

Each of the various statistical methods used to model effective connectivity begin by obtaining representative time series from anatomically or statistically identified ROIs (see Goncalves and Hall, 2003). Path diagrams fit by means of structural equation modeling (SEM) appear to be the most straightforward application and more common approach. Here, covariance patterns of contemporaneous blood-oxygen-level dependant (BOLD) time series illustrate brain functioning via directed pathways (McIntosh and Gonzalez-Lima, 1994). Outside of the general linear model approach, dynamic causal modeling (DCM) uses deterministic differential equations to assess how regions relate and estimate external modulation of connections (Friston, 2007). DCM attempts to include neuronal-hemodynamic activity in the model, making the model perhaps the most comprehensive to date (Sarty, 2007).

A third approach, vector (or "multivariate") autoregression (VAR), estimates the influence that data from ROIs at previous time points have on a given ROI's BOLD activity (Penny and Harrison, 2007). The use of VAR represents an important development in connectivity mapping for two reasons. One, BOLD activity contains sequential dependencies (Harrison et al., 2007) and VAR takes into account these autocorrelations (Shumway and Stoffer, 2006). Two, to be able to make causal inferences between ROIs, at minimum, temporal ordering must be established, i.e., a cause cannot occur later than its effect (Roebroeck et al., 2005). VARs identified by means of Granger causality offer an improvement upon DCM by not requiring a priori selection of directional associations among ROIs. Granger causality necessitates that including past information from one ROI offers a statistically unique contribution in explaining variance in a second ROI which is better than using solely the second ROI to predict itself (Goebel et al., 2003).

In what follows we review a fourth approach, the unified SEM approach of Kim et al. (2007) to model contemporaneous and sequential relationships among ROIs, and present several extensions. In particular, we introduce a new automatic search procedure to

* Corresponding author.
E-mail address: kgates@psu.edu (K.M. Gates).

1053-8119/$ – see front matter © 2010 Elsevier Inc. All rights reserved.
doi:10.1016/j.neuroimage.2009.12.117

identify optimal unified SEM models based on Lagrange multiplier testing. This automatic search procedure constitutes a powerful alternative to Granger causality testing in VAR modeling (Goebel et al., 2003). Additionally, the formal relationships among SEM path modeling, VAR, and unified SEM are explained and illustrated with applications to simulated and empirical data.

Methods

Unified SEM

Typically, SEM path modeling assesses contemporaneous relationships among ROIs. However, since biological mechanisms have sequential dependencies, connections estimated from solely contemporaneous path models may be biased (Harrison et al., 2007). In complement, VAR modeling assesses lagged relationships while neglecting to account for contemporaneous relationships among BOLD signals. Each approach could be improved by simultaneous consideration of both the contemporaneous and lagged effects. Kim et al. (2007) recently offered a solution which combines SEM path and VAR modeling into a "unified SEM". In this way a powerful integrated approach to the unbiased statistical estimation of fMRI connectivity mapping is obtained which allows for: (1) SEM path modeling of contemporaneous connectivities among ROIs while accommodating the presence of sequential dependencies, (2) VAR modeling of sequential connectivities while accommodating the presence of contemporaneous relationships among ROIs, and (3) simultaneous path and VAR modeling of contemporaneous and sequential relationships. In the present paper we provide an empirical demonstration that the statistical models underlying SEM path and VAR models can be derived as specific instances of unified SEM, for which an automatic search procedure exists. We then illustrate the relatedness of these approaches as well as the biases in parameter estimations that can occur when models fail to consider both contemporaneous and lagged effects.

Automatic optimal model search

Most current approaches for connectivity mapping require specification of connections among ROIs prior to estimation. Noting that optimal representations of underlying networks and effective connectivity may be best obtained using exploratory methods, a number of automated procedures have been developed to construct and identify the best fitting connectivity maps. For SEM models, the general approach is to specify, estimate, and compare all possible models (or at least a large selection of plausible models) to obtain the best fitting one (James et al., 2009; Zhuang et al., 2005). For VAR models, Granger causality tests are used to select models that identify regions that are driving or are driven by activation in a set of reference regions (Goebel et al., 2003). A striking and previously overlooked feature of the unified SEM is that an optimal model may be established without prior specification of contemporaneous and lagged paths. We introduce a new automatic search procedure for identifying optimal unified SEM models of fMRI data based on Lagrange multiplier tests. The method provides a robust alternative to the previous approaches in that it accommodates both contemporaneous and lagged effects, and, similar to the selection procedures used for Granger causality testing in VAR modeling (Goebel et al., 2003), model construction requires statistical improvement for each contemporaneous and lagged path.

Formal specification of SEM path models

Given a p-variate time series $\boldsymbol{\eta}(t)$ of ROI BOLD activities, $p>1$, path models can be fit which identify contemporaneous connectivity among these ROIs by means of SEM:

$$\boldsymbol{\eta}(t) = A\boldsymbol{\eta}(t) + \varepsilon(t) \tag{1}$$

where $\mathbf{A}$ is a (p,p) matrix with zeroes along the diagonal and $\varepsilon(t)$ denotes a p-variate residual series. Off-diagonal coefficients $\mathbf{A}_{ik}$, $i \neq k$, $i,k \in \{1,2,\ldots,p\}$, denote directed paths among ROIs $\boldsymbol{\eta}_i(t)$ and $\boldsymbol{\eta}_k(t)$. Let $\boldsymbol{\Sigma} = \mathrm{var}[\boldsymbol{\eta}(t)]$ and $\boldsymbol{\Delta} = \mathrm{var}[\varepsilon(t)]$ be the (p,p)-dimensional covariance matrices of $\boldsymbol{\eta}(t)$ and $\varepsilon(t)$, respectively. Please note that $\boldsymbol{\Delta}$ is a diagonal covariance matrix in order to guarantee unique parameter estimates. Then the path model is fitted to $\boldsymbol{\Sigma}$ as

$$\sum = \left(I_p - \mathbf{A}\right)^{-1} \Delta \left(I_p - A^{\mathrm{t}}\right)^{-1} \tag{2}$$

where $\mathbf{I}_p$ is the (p,p)-dimensional identity matrix and the superscript t denotes transposition. Model fits usually are obtained by means of the method of maximum likelihood given the assumption that observations are multivariately normally distributed (Penny and Harrison, 2007).

Formal specification of vector autoregression (VAR) models

VAR models can be used to obtain connectivity maps that identify sequential relationships among the BOLD activities of ROIs. Given a time series, $\boldsymbol{\eta}(t)$, representing $p>1$ ROIs of BOLD activities, sequential relationships among their BOLD activity can be modeled by means of a VAR of order q, VAR(q)

$$\boldsymbol{\eta}(t) = \Phi_1\boldsymbol{\eta}(t-1) + \ldots + \Phi_q\boldsymbol{\eta}(t-q) + \zeta(t), \tag{3}$$

where $\zeta(t)$ is a p-variate residual series.

Vector autoregression models can also be fit by means of SEM. Taking VAR(1) as an example, define $2p$-variate supervectors $\boldsymbol{\eta}^{\mathrm{t}} = [\boldsymbol{\eta}(t)^{\mathrm{t}}, \boldsymbol{\eta}(t+1)^{\mathrm{t}}]$ and $\zeta^{\mathrm{t}} = [\mathbf{0}^{\mathrm{t}}, \zeta(t+1)^{\mathrm{t}}]$, where $\mathbf{0}$ is the p-variate zero vector. In addition, define the $(2p,2p)$-dimensional matrix Φ consisting of four (p,p)-dimensional blocks Φ_{ik}, $i,k=1,2$: $\Phi_{11} = \mathbf{I}_p$, $\Phi_{12} = \Phi_{22} = \mathbf{0}_p$, where $\mathbf{0}_p$ is the (p,p)-dimensional zero matrix, and $\Phi_{21} = \Phi_1$, the (p,p)-dimensional matrix of autoregression coefficients in the VAR(1) $\boldsymbol{\eta}(t+1) = \Phi_1\boldsymbol{\eta}(t) + \zeta(t+1)$. Accordingly, the VAR(1) can be rewritten as the SEM

$$\boldsymbol{\eta} = \Phi\boldsymbol{\eta} + \zeta. \tag{4}$$

As is demonstrated below, reformulating VARs as SEMs opens up the possibility to make use of the option to automatically identify sequential relationships among ROIs using a recursive procedure offered by LISREL software (Jöreskog, 1997).

Formal specification of unified SEM

Kim et al. (2007) present a unified SEM approach to connectivity mapping that identifies both contemporaneous and sequential relationships among the BOLD activities of ROIs. Given a p-variate time series $\boldsymbol{\eta}(t)$ of BOLD activities associated with $p>1$ ROIs, we can combine Eqs. (1) and (3) into the following combination of path model and VAR(q):

$$\boldsymbol{\eta}(t) = A\boldsymbol{\eta}(t) + \Phi_1\boldsymbol{\eta}(t-1) + \ldots + \Phi_q\boldsymbol{\eta}(t-q) + \zeta(t). \tag{5}$$

Taking VAR(1) as an example, define the $2p$-variate supervectors $\boldsymbol{\eta}^{\mathrm{t}} = [\boldsymbol{\eta}(t)^{\mathrm{t}}, \boldsymbol{\eta}(t+1)^{\mathrm{t}}]$ and $\zeta^{\mathrm{t}} = [\mathbf{0}^{\mathrm{t}}, \zeta(t+1)^{\mathrm{t}}]$, where $\mathbf{0}$ is the p-variate zero vector. In addition, define the $(2p,2p)$-dimensional matrix $\mathbf{B}$ consisting of four (p,p)-dimensional blocks $\mathbf{B}_{ik}$, $i,k=1,2$: $\mathbf{B}_{11} = \mathbf{I}_p$, $\mathbf{B}_{12} = \mathbf{0}_p$, $\mathbf{B}_{21} = \Phi_1$, and $\mathbf{B}_{22} = \mathbf{A}$. Accordingly, the combined path model and VAR(1) can be rewritten as a unified SEM in LISREL notation as

$$\boldsymbol{\eta} = \mathbf{B}\boldsymbol{\eta} + \zeta. \tag{6}$$

This model allows for unbiased estimation of contemporaneous and lagged association by considering both simultaneously.

Unified SEM using automatic Lagrange multiplier testing

The reformulation of the combined path and VAR(q) as a SEM permits automatic identification of the minimum number of directed path coefficients for the Φ_k matrix, $k=1,\ldots,q$, and the **A** matrix using LISREL (Jöreskog and Sörbom, 1992). Using the generalized Lagrange multiplier test, the automatic search procedure constitutes an alternative to standard tests of Granger causality which is based on ratios of determinants of residual processes as described in Goebel et al. (2003). Lagrange multipliers help identify which path, if freed, would maximally improve the chi-squared goodness-of-fit when compared to the less parameterized model. The chi-squared goodness-of-fit statistic is the likelihood ration of the model against the observed covariance matrix. According to Chou and Bentler (1990), the Lagrange multiplier test is appropriate regardless of the type of parameter being tested. SEM presents an alternative to Granger causality applicable for both contemporaneous and sequential relationships.

LISREL can be programmed to automatically carry out Lagrange multiplier tests by iterative model estimation without prior specification of contemporaneous or lagged relationships. The automatic procedure starts by fitting an empty path model to the data. Next, generalized Lagrange multiplier tests indicate the directed path that, if added, would maximally improve the likelihood ratio test. The procedure automatically frees this path for estimation and fits the new model to the data, after which the generalized Lagrange multiplier test again determines the directed path which would maximally improve the likelihood ratio test if added to the path model. These steps are repeated until none of the modification indices reach statistical significance at a pre-specified alpha level (Jöreskog, 1997). Appendix A provides mathematical explanation of the Lagrange multiplier test.

Formal relationships among path modeling, VAR, and unified SEM

In this section the following formal key relationships will be considered: (a) each unified SEM can be transformed to an equivalent VAR; and (b) each VAR can be transformed to an equivalent unified SEM, using as an intermediate step SEM path modeling of the covariance matrix of the residual process in the VAR. The relationship between the unified SEM and VAR enables the use of the Lagrange multiplier test as an alternative to the widely accepted Granger causality tests in a model that considers both lagged and contemporaneous effects. For objective (b), we work in reverse to demonstrate how to acquire unbiased contemporaneous and sequential pathways using results from the VAR model. This may be a practical and equivalent alternative approach to the unified SEM for researchers. Notice that objective (b) allows for the a posteriori transformation of published results obtained by means of VAR modeling.

a) Transformation of unified SEM to an equivalent VAR. Given the unified SEM (Eq. (7)), which for clarity of presentation is truncated to include only lagged associations of order 1, consider the following transformation:

$$\begin{aligned}&\boldsymbol{\eta}(t+1) = A\boldsymbol{\eta}(t+1) + \boldsymbol{\Phi}_1\boldsymbol{\eta}(t) + \zeta(t+1)\rightarrow\\ &\boldsymbol{\eta}(t+1) = \left(I_p - A\right)^{-1}\boldsymbol{\Phi}_1\boldsymbol{\eta}(t) + \left(I_p - A\right)^{-1}\zeta(t+1)\end{aligned} \quad (7)$$

where $\mathbf{I}_p$ is the identity matrix, Φ_1 the autoregressive coefficient matrix, and **A** the coefficient matrix for contemporaneous paths. We define $(\mathbf{I}_p\text{-}\mathbf{A})^{-1}\Phi_1 = \Phi_1{}^*$ and $(\mathbf{I}_p\text{-}\mathbf{A})^{-1}\zeta(t) = \zeta^*(t)$. Then the right-hand side of Eq. (9) can be rewritten as $\boldsymbol{\eta}(t+1) = \Phi_1{}^*\boldsymbol{\eta}(t) + \zeta^*(t)$, which is a VAR(1).

For the unified SEM (Eq. (7)), $\mathrm{cov}[\zeta(t), \zeta(t)^t] = \boldsymbol{\Psi}$, which is a diagonal ($p$,$p$)-dimensional matrix. For the residual process $\zeta^*(t)$ in the equivalent VAR(1) model resulting from the above manipulation it holds that: $\mathrm{cov}[\zeta^*(t), \zeta^*(t)^t] = [(\mathbf{I}_p\text{-}\mathbf{A})^{-1}\boldsymbol{\Psi}(\mathbf{I}_p\text{-}\mathbf{A}^t)^{-1}]$, which represents a full covariance matrix associated with contemporaneous paths. This completes the formal transformation of a unified SEM model (Eq. (7)) to an equivalent VAR(1) model (Eq. (3)).

b) Transformation of a VAR to an equivalent unified SEM. Given is the VAR(1) $\boldsymbol{\eta}(t+1) = \Phi_1{}^*\boldsymbol{\eta}(t) + \zeta^*(t)$, using the same notation as in (a). As an intermediate step, the (p,p)-dimensional covariance matrix of the residual process $\zeta^*(t)$ is subjected to a SEM path analysis according to Eq. (2): $\mathrm{cov}[\zeta^*(t), \zeta^*(t)^t] = (\mathbf{I}_p\text{-}\mathbf{A})^{-1}\boldsymbol{\Psi}(\mathbf{I}_p\text{-}\mathbf{A}^t)^{-1}$. This SEM path analysis recovers the matrix **A** as well as the diagonal (p,p)-dimensional covariance matrix $\boldsymbol{\Psi}$ of the residual process $\zeta(t)$ in the unified SEM (Eq. (7)). In the final step, the $\Phi_1{}^*$ matrix is transformed by pre-multiplication with $(\mathbf{I}_p\text{-}\mathbf{A})$ in order to obtain the Φ_1 matrix in Eq. (7): $\Phi_1 = (\mathbf{I}_p\text{-}\mathbf{A})\Phi_1{}^*$. This concludes the transformation of a VAR into a unified SEM.

Results: Simulated data

Unified SEM with automatic search applied to simulated data

The present example will use the Lagrange multiplier test automatic procedure to estimate paths according to the unified SEM given by Eq. (8) on simulated data with $p=4$. The following parameter specifications produced the data:

$$A = \begin{bmatrix} 0 & 0 & .7 & 0 \\ 0 & 0 & .7 & 0 \\ 0 & 0 & 0 & 0 \\ 0 & 0 & .7 & 0 \end{bmatrix}$$

$$\Phi_1 = \begin{bmatrix} .8 & 0 & 0 & 0 \\ 0 & .8 & 0 & 0 \\ 0 & 0 & .8 & 0 \\ .5 & 0 & 0 & .8 \end{bmatrix}$$

The covariance matrix of $\zeta(t)$ is $\mathbf{I}_4$. The ROIs will be referred to as ROI 1, ROI 2, ROI 3, and ROI 4 in order from left to right across the matrices. For instance, the matrix specifications for **A** and Φ_1 created the data such that the coefficient for ROI 1 regressed on ROI 3 is .7 after taking into account the sequential relationships of .8 for ROI 1 on itself.

Appendix B contains a LISREL program for fitting the unified SEM using the automatic procedure. The LISREL user's reference guide (Jöreskog, 1997) provides detailed explanation of LISREL notation. The procedure conducts forward-selection in that it selects the best path accounting for the influence of previously selected paths, beginning with the empty path model. For this reason, paths estimated early in the iterative procedure may become non-significant as other paths are added. Recall that for the present example the **A** matrix is a 4×4 matrix in the lower right hand corner and Φ is the lower left hand 4×4 corner of the LISREL beta matrix.

Table 1 lists the parameters in the **B** matrix in Eq. (8) automatically freed in accordance with the iteratively applied Lagrange multiplier test. Of note, the program chose $\beta(8,5)$ to be the first contemporaneous parameter estimated. $\beta(8,5)$ corresponds to the coefficient for ROI 4 regressed on ROI 1 and was not specified in the unified SEM model used to create the data. However, ROI 4 at $t+1$ regressed on ROI 1 at t was specified in the unified SEM model (via the Φ matrix) used to create the data. Once the model selected this parameter to be estimated, the estimate for $\beta(8,5)$ became non-significant and remained non-significant ($t=0.33$) in the final model. Refitting the model with $\beta(8,5)$ constrained to zero resulted in a final model with an excellent fit ($\chi^2=7.01$, $p=.93$) that recovers the true parameter structure used to create the variables (Fig. 1). This exercise

Table 1
Fits for models found using the automatic Lagrange multiplier tests using simulated data example.

Model	Newly estimated Beta	χ^2	Significance
1	None	1393.52	$p<.001$
2	8,4	982.75	$p<.001$
3	6,3	711.39	$p<.001$
4	5,1	443.25	$p<.001$
5	8,5	321.55	$p<.001$
6	7,3	219.49	$p<.001$
7	5,7	130.16	$p<.001$
8	6,7	48.66	$p<.001$
9	8,7	33.13	$p<.001$
10	8,1	6.91	0.91

demonstrates that the automatic procedure can identify the true model without prior knowledge. We achieve this by first obtaining models in which each new path significantly improves the model and then trimming non-significant paths.

Equivalences among contemporaneous path model, VAR, and unified SEM

The formal relationships among contemporaneous path modeling, VAR, and unified SEM are explored here on the simulated data described above. We first estimate a VAR using the automatic search procedure. It is shown that parameter estimates from the VAR model contains biases arising directly from contemporaneous influences. In the process of recovering the unbiased unified SEM estimates for the lagged and contemporaneous paths using the formal relationships explicated above, the simulated data example also demonstrates the biases in contemporaneous paths resulting from models which do not account for lagged relationships. Then, with knowledge of the unbiased contemporaneous paths and the biased VAR estimates, we indicate how one arrives at unbiased estimates of both contemporaneous and sequential relationships. This final, crucial, step opens up the possibility for researchers to transform previously published VAR results into unbiased unified SEM estimates. Lagrange multiplier tests using the automatic search option in LISREL assisted in arriving at the final model fits for each step. The formal relationships among these three models are shown to hold when estimated in this manner, strengthening the claim that use of this automatic procedure constitutes a powerful approach in identifying optimal fMRI connectivity maps with no prior specification.

We now present the illustration of the transformation of a VAR to an equivalent unified SEM. These data were simulated according to a unified SEM as described above, but a VAR(1) is fitted to these data. Thus, some of the variation in these ROIs results from contemporaneous influence, similar to what has been demonstrated in empirical data (Kim et al., 2007). One can recover the coefficients found in a unified SEM by manipulating the results from the VAR analysis.

Accordingly, we estimated a VAR(1) model using the automatic procedure in LISREL described above. After iteratively estimating 10 models the final model containing 8 regression estimates (after trimming) has an excellent fit ($\chi^2=4.92$, $p=.77$):

$$\Phi_1^* = \begin{bmatrix} .79 & 0 & .51 & 0 \\ 0 & .81 & .45 & 0 \\ 0 & 0 & .70 & 0 \\ .55 & 0 & .54 & .78 \end{bmatrix}$$

Note that the coefficients in Φ_1* in the fitted VAR(1) do not follow the same pattern as those for the Φ_1 matrix in the unified SEM used to simulate the data. Apparently VAR models erroneously estimate some variance explained by contemporaneous influences as lagged relationships. This bias highlights the need for the unified SEM approach when attempting to make valid causal inferences.

From this analysis we acquire the $\zeta^*(t)$ residual covariance matrix which, as described above, contains the information regarding the covariance structure of the contemporaneous relations **A** as well as the covariance matrix of the residual process in the unified SEM. Using $\mathrm{cov}[\zeta^*(t), \zeta^*(t)^t]$ as input data for a SEM path model fit as intermediate step, we apply the automatic procedure to obtain the **A** matrix. The final model produces coefficient weights equivalent to those obtained for the **A** matrix in the unified SEM model underlying the simulated data (see Fig. 1) for ROI 1, 2, and 4 regressed on ROI 3. The path coefficients in **A** obtained in the intermediate SEM path analysis are, respectively: 0.72, 0.66, and 0.67.

In the final step, the Φ_1* in the fitted VAR(1) is transformed to obtain the Φ_1 matrix in the unified SEM: $\Phi_1=(\mathbf{I}_4\text{-}\mathbf{A})\Phi_1$*, using **A** obtained in the intermediate step. Table 2 displays the estimate of Φ_1 obtained in this final step, as well as (to aid comparison) the estimate of Φ_1 obtained in the fit of the unified SEM (above section). Comparison of (a) the Φ_1 matrix derived algebraically by fitting the VAR and using the resulting $\zeta^*(t)$ covariance matrix to estimate contemporaneous relations with (b) the Φ_1 matrix obtained with the unified SEM reveals nearly identical results. Any differences are likely due to rounding effects during the transformation procedure. Please note that this formal illustration of the relatedness among SEM path, VAR, and unified SEM necessitates having adequate power to appropriately model each component.

For completeness, SEM path diagrams of contemporaneous relations also were fit via the iterative search procedure to the original covariance matrix of the same simulated data: $\mathrm{cov}[\boldsymbol{\eta}(t), \boldsymbol{\eta}(t)^t]$.

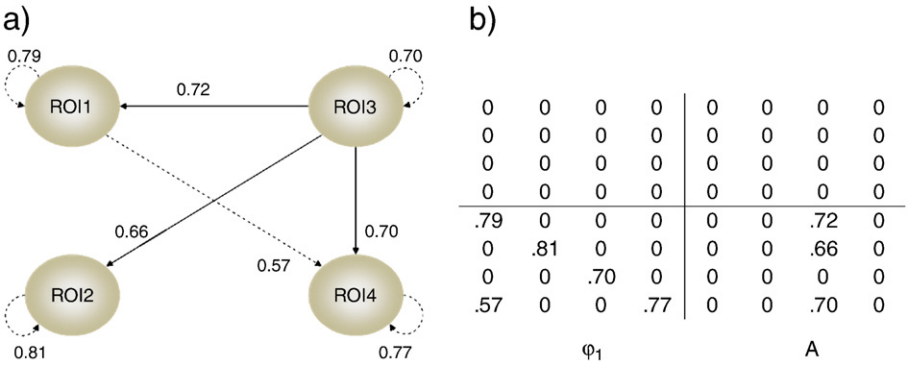

Fig. 1. Unified SEM diagram and corresponding beta matrix for simulated data example. *Note*: (a) Diagram of lag(1) relationships represented by dotted line and contemporaneous relationships denoted by solid lines. All relationships are significant at the $p<.05$ level. (b) Corresponding beta matrix obtained from LISREL.

Table 2
Φ_1 matrices obtained algebraically from VAR(1) and unified SEM approaches.

	ROI 1(t)	ROI 2(t)	ROI 3(t)	ROI 4(t)
	Φ_1 Obtained algebraically beginning with VAR(1)			
ROI 1($t+1$)	0.79	0.00	0.01	0.00
ROI 2($t+1$)	0.00	0.81	-0.01	0.00
ROI 3($t+1$)	0.00	0.00	0.70	0.00
ROI 4($t+1$)	0.55	0.00	0.07	0.78
	Φ_1 Obtained using unified SEM			
ROI 1($t+1$)	0.79	0.00	0.00	0.00
ROI 2($t+1$)	0.00	0.81	0.00	0.00
ROI 3($t+1$)	0.00	0.00	0.70	0.00
ROI 4($t+1$)	0.57	0.00	0.00	0.77

The matrix of contemporaneous paths thus obtained yields an unsatisfactory fit ($\chi^2 = 9.95$, $df = 1$):

$$\mathbf{A} = \begin{bmatrix} 0 & .5 & 0 & 0 \\ 0 & 0 & .7 & .2 \\ 0 & 0 & 0 & 0 \\ 1.7 & 0 & 0 & 0 \end{bmatrix}$$

Note that the contemporaneous model estimated from the original covariance matrix contains phantom paths which do not exist given the specifications used to simulate the data. Importantly, the contemporaneous model estimated using the residual covariance matrix from the VAR model arrived at appropriate coefficient estimates given the covariance structure of the original covariance matrix obtained directly from the data.

Methods and materials: Empirical data

In what follows we demonstrate the utility of the automatic search procedure for unified SEM first on an individual's fMRI BOLD activity. Next, we apply this method to a group to demonstrate feasibility at this level. Data were drawn from a larger study which examined working memory functioning among healthy controls and traumatic brain injured subjects. Subjects completed the *n-back* task during acquisition, a task widely used in the cognitive neurosciences to examine working memory functioning (see D'Esposito et al., 1998; Smith and Jonides, 1999; Wagner et al., 2001). All subjects used in the present analysis were healthy controls. The subject used in the individual analysis was a 22 year-old male. This subject was included in the group analysis ($n = 4$; 75% female; all Caucasian), for which there was a mean age of 31 (SD = 13.0, range = 21–49).

MRI data were collected using a Philips 3 T system and a 6-channel SENSE head coil (Philips Medical Systems, Best, The Netherlands). First, 3-D high resolution T1-weighted MPRAGE images were acquired for presenting functional activations with the following parameters: repetition time (TR) 9.9 ms, echo time (TE) of 4.6 ms, and flip angle (FA) 8° with a $240 \times 204 \times 150$ mm^3 field of view (FOV). Echo planar imaging (EPI) was used for functional imaging. Imaging parameters for EPI consisted of: TR 2000 ms, TE 30 ms, FA 89°, FOV 230×230 mm^2, 80×80 acquisition matrix, and 34 4-mm thick axial slices with no gap between slices.

Data processing was conducted using SPM5 (Friston et al., 1995) software and included realignment of functional data to the first functional image using affine transformation (Ashburner et al., 1997). Functional images were also co-registered to the T1 MPRAGE and all data were normalized using a standardized T1 template from the Montreal Neurological Institute, MNI, using a 12 parameter affine approach and bilinear interpolation. Following normalization, scans were smoothed with a Gaussian kernel of $8 \times 8 \times 10$ mm^3. The BOLD response during task simulation was examined by comparing BOLD signal change during 20-s experimental blocks against baseline (i.e., fixation) using a *t*-test, a minimum cluster level of 10, and a statistical threshold set at $p < .001$. Data from the peak voxels in selected ROIs on the right and left side were extracted using the MarsBar toolbox (Brett et al., 2002).

Results: Empirical data

Having demonstrated the ability for the automatic search procedure utilizing Lagrange multiplier tests to correctly identify the model, we next applied this procedure to empirical data to illustrate the applicability of this approach for modeling both individuals and groups. We first obtained a connectivity map for an individual and then a separate one for the group. Both maps ascertained the coordinated network underlying working memory performance elicited from the task described above. Research examining basic information processing (e.g., working memory) consistently find increased activity in the anterior cingulated cortex (ACC) and prefrontal cortex (PFC) in clinical and healthy samples (Hillary et al., 2006; Hillary, 2008). Accordingly, data from these areas on the left and right hemispheres were collected for a total of four time series of peak voxel activity (LACC, LPFC, RACC, RPFC) processed by SPM5 as described above.

Individual analysis

The same program employed for the simulated data which used LISREL's automatic search procedure (Appendix B) was then applied to data obtained from an individual subject. Table 3 displays the chi-square test of goodness-of-fit associated with each β parameter newly freed in accordance with the Lagrange multiplier test. The path representing LACC1 (left ACC at $t+1$) regressed on RPFC1 (right PFC at $t+1$) became non-significant ($t = -.05$) once the autoregressive influence for LACC (LACC at time) entered the model at the 14th iteration. Trimming the model by constraining this parameter to zero and refitting resulted in a final model with an excellent fit ($\chi^2 = 14.41$, $p = .16$, Standardized RMR = .02, NNFI = .99, CFI = 1.00; Fig. 2). The autocorrelation function (ACF) for each region confirmed the appropriateness of the model as they evidenced white noise processes in the errors with no more significant lagged correlations than would be expected by chance (Fig. 2).

Group analysis

For the group analysis, we pooled the individual covariance matrices to arrive at a group covariance matrix representing average

Table 3
Fits for models found using the automatic Lagrange multiplier tests using empirical individual example.

Model	Newly estimated Beta	χ^2	Significance
1	None	677.56	$p < .001$
2	LPFC1<-RPFC1	517.35	$p < .001$
3	LACC1<-LPFC1	390.10	$p < .001$
4	RPFC1<-RPFC	282.33	$p < .001$
5	RACC1<-LACC1	222.25	$p < .001$
6	RACC1<-RACC	185.31	$p < .001$
7	RPFC1<-LACC	158.62	$p < .001$
8	RPFC1<-RACC1	107.74	$p < .001$
9	RPFC1<-RACC	88.59	$p < .001$
10	RPFC1<-LPFC1	69.21	$p < .001$
11	LACC1<-RPFC1	57.79	$p < .001$
12	RPFC1<-LPFC	50.10	$p < .001$
13	LACC1<-LPFC	44.64	$p < .001$
14	LACC1<-LACC	14.40	$p = .11$
15	LACC1<-RPFC	6.97	$p = .54$

Note. ACC = anterior cingulated cortex and PFC = prefrontal cortex. The prefixes of L = left and R = right. Abbreviations ending in "1" denote the time series at one scan in the future.

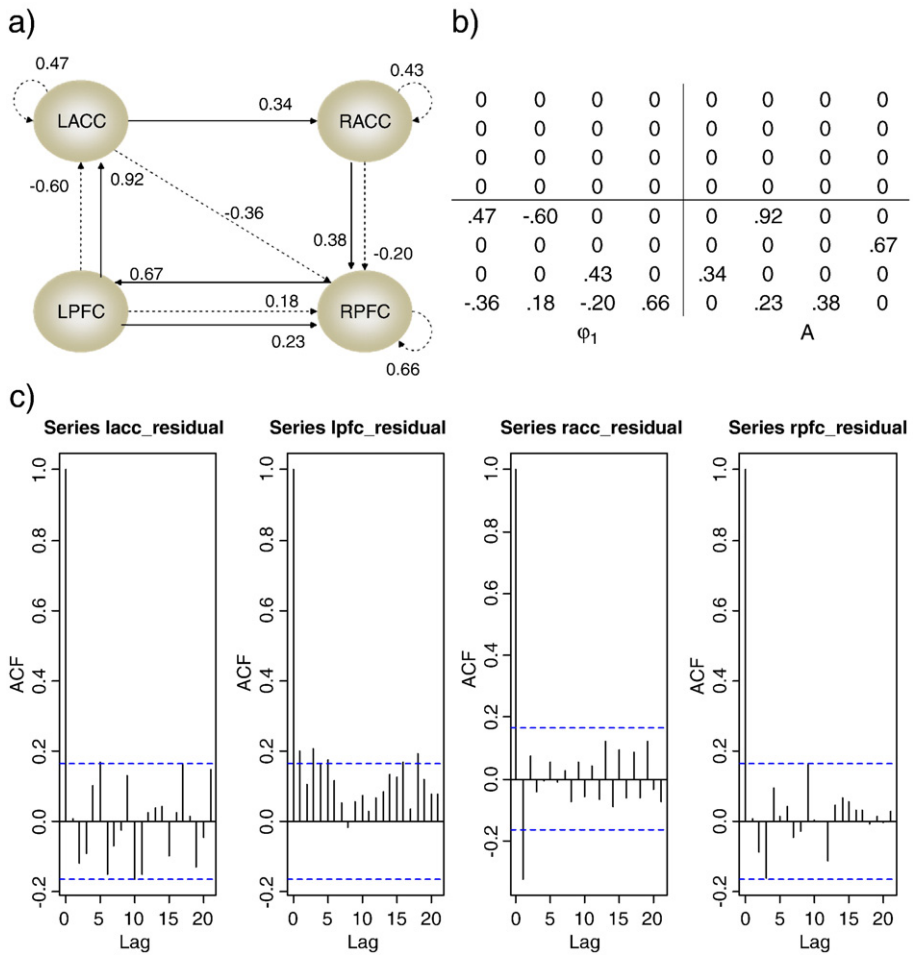

Fig. 2. Unified SEM diagram and corresponding beta matrix for empirical individual example. *Note*: (a) Diagram of lag(1) relationships represented by dotted line and contemporaneous relationships denoted by solid lines. All relationships are significant at the $p<.05$ level. ACC = anterior cingulated cortex and PFC = prefrontal cortex. The prefixes of L = left and R = right. (b) Corresponding beta matrix obtained from LISREL. (c) Autocorrelation (ACF) plots for each region's residuals indicating white noise processes.

relations among the ROIs with a lag of one. Again we applied the program offered in Appendix B. Table 4 displays the chi-square test of goodness-of-fit associated with each β parameter newly freed in accordance with the Lagrange multiplier test. All estimated beta coefficients remained significant in the final model acquired using the automatic search procedure (Fig. 3) and the model had an excellent fit ($\chi^2 = 9.14$, $p = .42$; Standardized RMR = .01, NNFI = 1.00, CFI = 1.00). The autocorrelation function (ACF) for each region confirmed the appropriateness of the model as they evidenced white noise processes (Fig. 3).

Table 4
Fits for models found using the automatic Lagrange multiplier tests using empirical group example.

Model	Newly estimated Beta	χ^2	Significance
1	None	1385.54	$p<.001$
2	RPFC1<-RPFC	1029.70	$p<.001$
3	LPFC1<-LPFC	737.36	$p<.001$
4	RACC1<-RACC	544.83	$p<.001$
5	LACC1<-RACC1	365.63	$p<.001$
6	RPFC1<-LPFC1	256.61	$p<.001$
7	LPFC1<LACC1	158.93	$p<.001$
8	LACC1<-LACC	100.11	$p<.001$
9	RACC1<-RPFC1	57.28	$p<.001$
10	RPFC1<-LACC	42.78	$p<.001$
11	LPFC1<-LACC	31.68	$p<.001$
12	LPFC1<-RACC	22.54	$p=.020$
13	RACC1<-RPFC	13.26	$p=.21$
14	RACC1<-LPFC1	9.14	$p=.42$

Note. ACC = anterior cingulated cortex and PFC = prefrontal cortex. The prefixes of L = left and R = right. Abbreviations ending in "1" denote the time series at one scan in the future.

Discussion

Kim et al. (2007) present an approach, the unified SEM, for assessing effective connectivity in ROIs that resolves concerns arising from other procedures. First, the unified SEM allows for estimation of contemporaneous relations controlling for sequential dependencies which offers an improvement upon path modeling. Second, the unified SEM obtains VAR estimates of lagged relationships after controlling for contemporaneous effects, improving upon prior models of effective connectivity. The unified SEM achieves these objectives by simultaneously estimating contemporaneous and lagged relationships.

A previously overlooked benefit of the unified SEM presents itself when using LISREL software for estimation. Lagrange multiplier tests conducted in an automatic procedure implemented in LISREL can be used to select the most desirable directional paths. The program iteratively selects in order paths that provide the greatest improvement to the likelihood ratio tests. In this way, the automatic procedure applied to the unified SEM is comparable to Granger causality in VAR analysis. Because the procedure conducts forward-selection (i.e., selects the best path accounting for the influence of previously selected paths), we suggest a posteriori trimming of non-significant paths. The final model can then be re-estimated with the significant

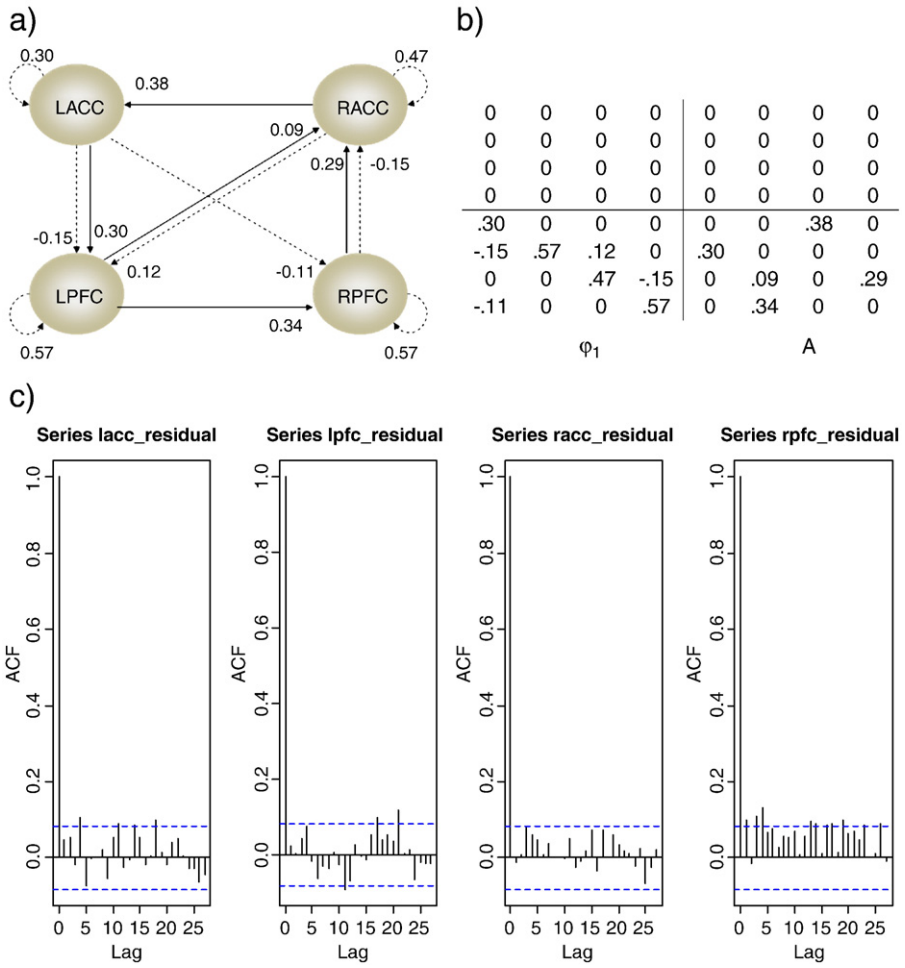

Fig. 3. Unified SEM diagram and corresponding beta matrix for empirical group example. *Note*: (a) Diagram of lag(1) relationships represented by dotted line and contemporaneous relationships denoted by solid lines. All relationships are significant at the $p<.05$ level. ACC = anterior cingulated cortex and PFC = prefrontal cortex. The prefixes of L = left and R = right. (b) Corresponding beta matrix obtained from LISREL. (c) Autocorrelation (ACF) plots for each region's residuals indicating white noise processes.

parameters estimated freely and all other paths constrained to zero. In this manner, the program derives directional contemporaneous and lagged paths that best match the data without necessitating prior knowledge or theory of the relationships.

Finally, as another important addendum to the Kim et al. (2007) article the present paper explicated the formal relationships among SEM path modeling, VAR, and unified SEM. We used simulated data to show how a fitted unified SEM can be transformed into an equivalent VAR, and vice versa. In the process of demonstrating these relationships, the biases which occur when estimating contemporaneous or lagged relationships without simultaneously considering both surfaced. While a general form of the model was explicated here, the model can be extended to include greater lags and more regions of interest.

The ability to use a practical automatic search procedure for unified SEM comes at an excellent time for researchers interested in establishing connectivity maps of ROIs derived from fMRI data. The state of fMRI research is quickly moving towards wanting to know not just which ROIs become active during a task, but how the brain orchestrates information processing among identified ROIs. The ability for statistically drawn connectivity maps could greatly inform burgeoning theories regarding effective connectivity.

Appendix A. Lagrange multiplier test

If data y generated by a joint density function $f(y, \theta^0)$ under the null hypothesis and by $f(y, \theta)$ with $\theta \in R^k$ under the alternative, the Lagrange multiplier test maximizes the log-likelihood to the constraint $\theta = \theta^0$. Letting H be the Lagrangian and defining $L(\theta, y)$ as the log of $f(y,\theta)$:

$$\mathrm{H} = L(\theta, y) - \lambda^{\mathrm{t}}\left(\theta - \theta^0\right)$$

with first order conditions $\partial L/\partial\ \theta\ =\ \lambda$ and $\mathrm{B} = \theta^{\ 0}$. The score, defined as:

$$s(\theta, y) = \partial L(\theta, y) / \partial\theta,$$

is set to zero under maximum likelihood estimation and is equal to λ.

The distribution of the score under the null will have a mean of zero and variance $\Upsilon(\theta^0)T$ where T is the time or length of the series. The statistic:

$$\xi_{\mathrm{LM}} = s^{\mathrm{t}}(\theta, y)^{\mathrm{t}} Y^{-1}\left(\theta^0\right) s(\theta, y) / T,$$

will have a χ^2 distribution with k degrees of freedom. If ξ_{LM} is high, the constraint that the model with the extra parameter estimated equals the null (or less parameterized model) may be rejected (Engle, 1984). It follows from Eq. (8) in Sörbom (1989) that the current version of LISREL's modification index is equivalent to the Lagrange multiplier test based on ξ_{LM}.

Appendix B

Sample LISREL program for conducting unified SEM using the automatic Lagrange multiplier test search procedure.

```
da no=150 ni=8 ma=cm
cm sy fi=cov.doc
mo ny=8 ne=8 ly=id te=ze be=fu,fi ps=sy,fi
pa ps
1
1 1
1 1 1
1 1 1 1

0 0 0 0  1
0 0 0 0  0 1
0 0 0 0  0 0 1
0 0 0 0  0 0 0 1

! the below "nf" commands ensure that only paths in the ϕ and A
! matrices are considered by the Lagrange multiplier tests.

nf ps(6,5) ps(7,5) ps(7,6)
nf ps(8,5) ps(8,6) ps(8,7)
nf ps(5,1) ps(5,2) ps(5,3) ps(5,4)
nf ps(6,1) ps(6,2) ps(6,3) ps(6,4)
nf ps(7,1) ps(7,2) ps(7,3) ps(7,4)
nf ps(8,1) ps(8,2) ps(8,3) ps(8,4)
nf be(1,1) be(2,1) be(3,1) be(4,1)
nf be(1,2) be(2,2) be(3,2) be(4,2)
nf be(1,3) be(2,3) be(3,3) be(4,3)
nf be(1,4) be(2,4) be(3,4) be(4,4)
nf be(1,5) be(1,6) be(1,7) be(1,8)
nf be(2,5) be(2,6) be(2,7) be(2,8)
nf be(3,5) be(3,6) be(3,7) be(3,8)
nf be(4,5) be(4,6) be(4,7) be(4,8)
ou am sl=5
```

Acknowledgment

This work was supported by a National Science Foundation grant (0852147).

References

Ashburner, J., Neelin, P., Collins, D.L., Evans, A., Friston, K., 1997. Incorporating prior knowledge into image registration. NeuroImage 6 (4), 344–352.
Brett, M., Anton, J.L., Valabregue, R., Poline, J.B., 2002, Junee. Region of interest analysis using an SPM toolbox [abstract]. Presented at the 8th International Conference on Functional Mapping of the Human Brain. Sendai, Japan.
Chou, C-P., Bentler, P.M., 1990. Model modification in covariance structure modeling: a comparison among Likelihood Ratio, Lagrange Multiplier, and Wald tests. Multivariate Behav. Res. 25, 115–136.
D'Esposito, M., Aguirre, G.K., Zarahn, E., Ballard, D., Shin, R.K., Lease, J., 1998. Functional MRI studies of spatial and nonspatial working memory. Cogn. Brain Res. 7 (1), 1–13.
Engle, R.F., 1984. Wald, likelihood ratio, and Lagrange multiplier tests in Econometrics. In: Griliches, Z., Intriligator, M.D. (Eds.), Handbook of Econometrics, II. Amsterdam, North Holland, pp. 775–826.
Friston, K.J., 2007. Dynamic causal modeling. In: Friston, K.J., Ashburner, J.T., Kiebel, S.J., Nichols, T.E., Penny, W.D. (Eds.), Statistical Parametric Mapping: The Analysis of Functional Brain Images. Academic Press, Amsterdam, pp. 541–560.
Friston, K.J., Holmes, A.P., Poline, J.B., Grasby, P.J., Williams, S.C., Frackowiak, R.S., Turner, R., 1995. Analysis of fMRI time-series revisited. NeuroImage 2, 45–53.
Friston, K.J., Stephan, K., 2007. Modeling brain responses. In: Friston, K.J., Ashburner, J.T., Kiebel, S.J., Nichols, T.E., Penny, W.D. (Eds.), Statistical Parametric Mapping: The Analysis of Functional Brain Images. Academic Press, Amsterdam, pp. 32–45.
Goebel, R., Roebroeck, A., Kim, D.S., Formisano, E., 2003. Investigating directed cortical interactions in time-resolved fMRI data using vector autoregressive modeling and Granger causality mapping. Magn. Reson. Imaging 21, 1251–1261.
Goncalves, M.S., Hall, D., 2003. Connectivity analysis with SEM: an example of the effects of voxel selection. NeuroImage 20, 1455–1467.
Harrison, L., Stephen, K., Friston, K., 2007. Effective connectivity. In: Friston, K.J., Ashburner, J.T., Kiebel, S.J., Nichols, T.E., Penny, W.D. (Eds.), Statistical Parametric Mapping: The Analysis of Functional Brain Images. Academic Press, Amsterdam, pp. 508–521.
Hillary, F.G., 2008. Neuroimaging of working memory dysfunction and the dilemma with brain reorganization hypotheses. J. Int. Neuropsychol. Soc. 14 (4), 526–534.
Hillary, F.G., Genova, H.M., Chiaravalloti, N.D., Rypma, B., DeLuca, J., 2006. Prefrontal modulation of working memory performance in brain injury and disease. Hum. Brain Mapp. 27, 837–847.
James, G.A., Kelley, M.E., Craddock, R.C., Hotzheimer, P.E., Dunlop, B.W., Nemeroff, C.B., Mayberg, H.S., Hu, X.P., 2009. Exploratory structural equation modeling of resting-state fMRI: applicability of group models to individual subjects. NeuroImage 45, 778–787.
Jöreskog, K.G., 1997. LISREL 8: User's Reference Guide. Chicago: Scientific Software International, Inc.
Jöreskog, K.G., Sörbom, D., 1992. LISREL. Scientific Software International, Inc.
Kim, J., Zhu, W., Chang, L., Bentler, P.M., Ernst, T., 2007. Unified structural equation modeling approach for the analysis of multisubject, multivariate functional MRI data. Hum. Brain Mapp. 28, 85–93.
McIntosh, A.R., Gonzalez-Lima, F., 1994. Structural equation modeling and its application to network analysis in functional brain imaging. Hum. Brain Mapp. 2, 2–22.
Penny, W., Harrison, L., 2007. Multivariate autoregressive models. In: Friston, K.J., Ashburner, J.T., Kiebel, S.J., Nichols, T.E., Penny, W.D. (Eds.), Statistical Parametric Mapping: The Analysis of Functional Brain Images. Academic Press, Amsterdam, pp. 534–540.
Roebroeck, A., Formisano, E., Goebel, R., 2005. Mapping directed influence over the brain using Granger causality and fMRI. NeuroImage 25, 230–242.
Sarty, G.E., 2007. Computational Brain Activity Maps from fMRI Time-Series Images. Cambridge University Press, New York.
Shumway, R.H., Stoffer, D.S., 2006. Time Series Analysis and Its Applications with R Examples. Springer, New York.
Smith, E.E., Jonides, J., 1999. Storage and executive processes in the frontal lobes. Science 283 (5408), 1657–1661.
Sörbom, D., 1989. Model modification. Psychometrika 54, 371–384.
Wagner, A.D., Maril, A., Bjork, R.A., Schacter, D.L., 2001. Prefrontal contributions to executive control: fMRI evidence for functional distinctions within lateral prefrontal cortex. NeuroImage 14 (6), 1337–1347.
Zhuang, J., LaConte, S., Peltier, S., Zhang, K., Hu, X., 2005. Connectivity exploration with structural equation modeling: an fMRI study of bimanual motor coordination. NeuroImage 25, 462–470.